

## Impact Testing to Quantify Structural Damage in Reinforced Concrete Frames

I. Villemure<sup>1</sup>, C.E. Ventura<sup>2</sup> and R.G. Sexsmith<sup>3</sup>

### ABSTRACT

Forced vibration tests were performed on five 0.45 scale reinforced concrete bridge bents to find relationships between their dynamic characteristics and structural degradation. The first bent specimen tested was modelled to match the original design of an actual bent of the Oak Street Bridge in Vancouver. The other four specimens modelled retrofitted versions of the same bent. Each bent was subjected to sequences of lateral slow cyclic loading, which was increased for each sequence until failure of the bent occurred. Between these sequences, corresponding to increasing levels of structural damage, forced vibration tests were performed on the bents. Frequency domain analyses of the experimental data were performed in order to identify dynamic characteristics of each bent at each level of structural damage. The sensitivity of natural frequencies and damping ratios to structural damage was investigated as part of this study. The decreasing fundamental frequencies were related to the increasing ductility levels, the latter reflecting the structural damage of the bents. Sensitivity analyses were also performed to relate damping ratio changes to ductility levels imposed on the specimens.

### INTRODUCTION

A seismic retrofit program for bridges has been undertaken by the B.C. Ministry of Transportation and Highways. Under this program, tests of modal bents from the Oak Street Bridge in Vancouver were conducted in the Structures Laboratory of the University of British Columbia. Five specimens were tested under lateral loading sequences. The first specimen was modelled to match the original design of the Oak Street Bridge while the other four specimens modelled retrofitted schemes of the original bent. Each specimen was brought to complete destruction or to very high damage level.

Several nondestructive techniques have been developed to assess properties of civil engineering structures, some of these being X-ray techniques, acoustic emission and ultrasonics. The use of modal testing represents another mean of damage detection in structures. Two types of vibration testing were performed on the bents: impact testing with an instrumented hammer and ambient vibration testing. Between each level of damage, vibration testing of the specimen was performed to assess its dynamic behaviour. Data obtained from these tests were used to investigate sensitivity of frequency and damping ratio to structural degradation.

---

<sup>1</sup>Graduate student, University of British Columbia

<sup>2</sup>Assistant Professor, University of British Columbia

<sup>3</sup>Associate Professor, University of British Columbia

## 1.0 DESCRIPTION OF SPECIMENS

The 0.45 scale specimens consisted of reinforced concrete bridge bents, a cap beam supported by two columns. All specimens had overall scale dimensions of 3.53m in width by 2.75m in height (see Figure 2). In order to model a hinged bearing support at the bottom end of the columns, only half of the columns were modelled (the bending moment being zero at the middle point).

The first specimen tested (S1) was modelled to match the original design of an actual bent of the bridge. The retrofit of the second specimen (S2) consisted of coring the cap beam along its longitudinal axis and grouting two post-tensioned tendons in the cap beam. Both the cap beam and the columns were retrofitted on specimen 3 (S3). The middle part of the cap beam was retrofitted by vertically anchoring a beam under it while 1/4" steel jackets were added to the columns. Retrofit scheme of specimen 4 (S4) also included retrofit of both the cap beam and the columns. Vertical prestressing, in the middle part only, as well as longitudinal prestressing were used to retrofit the cap beam. 1/4" steel jackets were also used to retrofit the S4 columns. A fibreglass retrofit technique was used on specimen 5 (S5). These epoxy-glued membranes were fixed on both the columns and the middle part of the cap beam (see Figure 1). The retrofit also included external prestressing along the longitudinal axis of the cap beam.

## 2.0 DESCRIPTION OF EXPERIMENTAL PROCEDURE

### 2.1. Vertical and lateral loading

Scale loads of 169 kN were imposed at five locations on the bent in order to simulate the superstructure dead load. These loads were applied through a system of hydraulic jacks and Dywidag bars pulling down on the bent. Lateral loading was applied through a horizontal jack along a longitudinal axis at the deck level above the bent. A loading truss was designed to transfer this lateral load at a level that would simulate the deck inertial loads. More details on the test setup are available in Anderson et al. (1995). Each sequence, corresponding to increasing levels of damage, consisted of three complete cycles. Displacement ductility was used to quantify structural damage of the bents. Typical ductility values were 0.75, 1.0, 1.5, 2.0, 3.0, 4.0, 6.0, 9.0 and 12.0. Ductility level  $u=12.0$  represented an upper ductility limit imposed by the experimental hinged bearing supports. Due to this limitation of the experimental setup, complete failure of specimen S5 was not achieved at  $u=12.0$ . Specimens S1 and S2 reached failure at low ductility levels. Table 1 summarizes failure mode and maximum ductility level for each specimen.

Table 1. Details on failure behaviour

Specimen	Failure Mode	Maximum Ductility Level
S1	shear failure in the cap beam	$\mu = 4.0$
S2	shear failure in the north column	$\mu = 6.0$
S3	failure by hinging in the beam/column joints	$\mu = 12.0$
S4	failure by hinging in the beam/column joints	$\mu = 12.0$
S5	high damage caused by spread cracking in the columns	$\mu = 12.0$

## 2.2. Forced vibration testing

Two types of vibration tests were performed on the bents: impact testing and ambient vibration testing. Impact testing was the main vibration technique investigated in this study. The ambient vibration technique was used for results validation purposes (refer to Felber, 1993 and Schuster, 1994 for details on the procedure). These vibration tests were performed before the specimen had suffered any structural damage and after each ductility level sustained by the bent.

Impacts were induced by an impulse hammer that includes an integral piezoelectric force sensor to measure the force applied. Hammer impacts were input on the structure at three different locations and three different directions (see Figure 2). The directions of impact corresponded to the three principal orthogonal directions: longitudinal direction (in the plane of the bent and parallel to the cap beam), transverse direction (perpendicular to the plane of the bent) and the vertical direction (in the plane of the bent and parallel to the columns). Four sets of impact were induced per ductility level. Each set of impacts consisted of four consecutive hammer blows. Two sets of hammer impact were induced along the longitudinal axis of the cap beam (direction of the lateral loading cycles). The two other sets were in the transverse and vertical directions. The longitudinal impacts were implemented at the end of the cap beam, while the transverse and vertical impacts were input in the middle part of the cap beam (see Figure 2). Table 2 summarizes the experimental measurement characteristics for each specimen.

Table 2. Impact test characteristics

Specimen	Time Resolution [sec]	Frequency Resolution [Hz]	Averaged Impact Peak [g]
S1	0.005	0.049	0.066
S2	0.005	0.049	0.066
S3	0.001	0.061	0.173
S4	0.001	0.061	0.106
S5	0.001	0.061	0.118

Two setups of accelerometers were used to measure the induced vibrations on the bents since only eight sensors were available (see Figure 2). For preliminary testing, vibrations from setup no.1 and setup no.2 were measured. Together, these two setups recorded vibrations at six selected locations: four on the top of the cap beam and two on the sides of the columns. To accelerate the procedure, only accelerometers from setup no.1 were used during the actual lateral loading cycles. Figure 2 shows that accelerometers measured motions in three principal orthogonal directions.

## 3.0 FREQUENCY ANALYSIS

### 3.1 Data analysis

Although vibrations were measured in three orthogonal directions, only the lateral direction results are discussed in this paper. Analysis of frequency was limited to the first longitudinal mode. Typical time

histories induced in longitudinal direction are shown in Figure 3 for different ductility level. The frequency response function (FRF) was used to determine the natural frequency at each damage level. The FRF relates the output signal to the input signal. In this study, the response of the longitudinal sensor on the cap beam was taken as the output. The hammer impulse in the longitudinal direction represented the input signal (see Figure 2). Typical FRF plots evaluated are shown in Figure 4. Peaks in the FRF indicate possible natural frequencies of the system under study. The ambient vibration analysis was performed using the programs U2, V2 and P2 (EDI Ltd, 1994). Results obtained are discussed below.

### 3.2 Results

FRF's were evaluated for all specimens at each ductility levels (Villemure, 1995) using a program developed at U.B.C. by Horyna (1995). Figure 4 clearly shows the peak associated with the first longitudinal mode. The preliminary frequencies vary between 18.9 Hz (S5) and 22.3 Hz (S3) while the failure frequencies fluctuate between 12.9 Hz (S1) and 17.2 Hz (S5). The smooth trend of the graph depended on the sampling frequency used to record the vibration responses. The frequency sensitivity to structural damage is shown in Figure 5. Generally, all specimens show decreasing frequency with increasing damage or ductility level. However, the rate of decay varies for each specimen. Specimens S2 and S5 present some irregularities. For certain ductility levels, the longitudinal frequency increases with increasing damage. These anomalies are currently being investigated. These results correlate with the frequencies obtained from ambient data analysis.

## 4.0 DAMPING ANALYSIS

### 4.1 Data analysis

Two methods were used to assess damping sensitivity to structural damage. Specimens were first assumed to behave with viscous damping. In that case, damping force is proportional to the frequency of vibration and increases with the latter (Humar, 1990). High frequencies of typical response signals were filtered to remove contribution of higher modes. Then, damping ratios were evaluated using the logarithm decrement method. The second method assumed structural (or hysteretic) damping. This type of damping is not dependent of frequency or it can decrease with increasing frequency (Humar, 1990). Results obtained are summarized in the following section.

### 4.2 Results

Damping ratios evaluated from viscous damping assumption show no particular trend with increasing damage level (see Figure 6). By reference to Figure 3, one can observe that the exponential decay for the larger ductility levels is affected by modulation in the signals. This could explain the non-coherent trend of damping ratio evaluated with viscous damping. Structural damping calculations were based on the hysteresis loops obtained from the cyclic loading sequences. Evaluated damping ratios increased with the increasing ductility level (see Figure 7). Considering that this type of damping is closely associated with internal friction, increasing damping ratios were expected to correlate with increased cracking of the specimen.

## CONCLUSIONS

Impact testing was used as a mean of damage assessment in reinforced concrete frames. Experimental data were analyzed to study sensitivity of frequency and damping ratio to structural deterioration. Frequency domain analyses were performed to identify the first longitudinal frequency. Generally, all specimens showed decreasing frequency with increasing ductility levels. Damping ratio sensitivity was analyzed with two types of damping. No particular coherent trend yielded from the viscous damping study. Calculations were based on the logarithmic decrement method. Structural damping evaluated with hysteresis loops provided coherent increasing damping with increasing structural damage.

## ACKNOWLEDGEMENTS

The financial support of the Natural Science and Engineering Research Council (N.S.E.R.C.) of Canada is gratefully acknowledged. This includes a Postgraduate Scholarship as well as Research Grants awarded to both Dr. C.E. Ventura and Dr. R.G. Sexsmith. The research was also made possible by financial support of the Ministry of Transportation and Highways of British Columbia. I would like to thank all the students from U.B.C. who provided assistance during the tests.

## REFERENCES

- Anderson et al. (1995), "Tests of alternate seismic retrofits of Oak Street Bridge", 7<sup>th</sup> Canadian Conference on Earthquake Engineering.
- Casas, J.R., Aparicio, A.C. (1994), "Structural damage identification from dynamic-test data", Journal of Structural Engineering, Vol. 120, No.8.
- Ewins, D.J. (1984), "Modal testing: theory and practice", John Wiley and Sons, New York, 269 pages.
- Felber, A.J. (1993), "Development of a hybrid evaluation system", Ph.D. Thesis, University of British Columbia, 275 pages.
- Fladung, W.A., Brown, D.L. (1993), "Multiple reference impact testing", 11<sup>th</sup> IMAC, pp. 1221-1229.
- Horyna, T. (1995), Master Thesis (to be published), University of British Columbia.
- Humar, J.L. (1990), "Dynamics of structure", Prentice Hall, New Jersey, pp. 168-194.
- Schuster, N. D. (1994), "Dynamic characteristics of a 30 storey building during construction detected from ambient vibration measurements", Master Thesis, University of British Columbia, 215 pages.
- Villemure, I. (1995), Master Thesis (to be published), University of British Columbia.

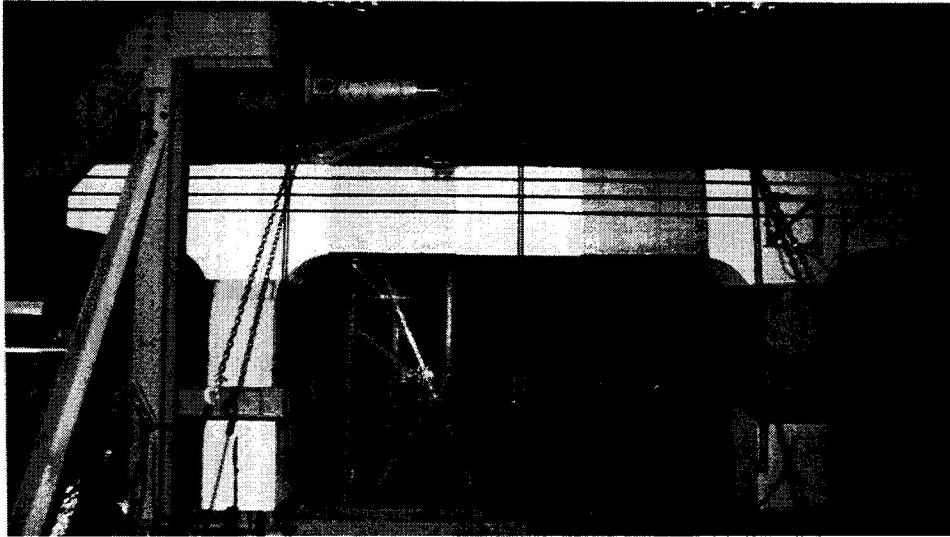


Figure 1. Specimen S5 ready for testing

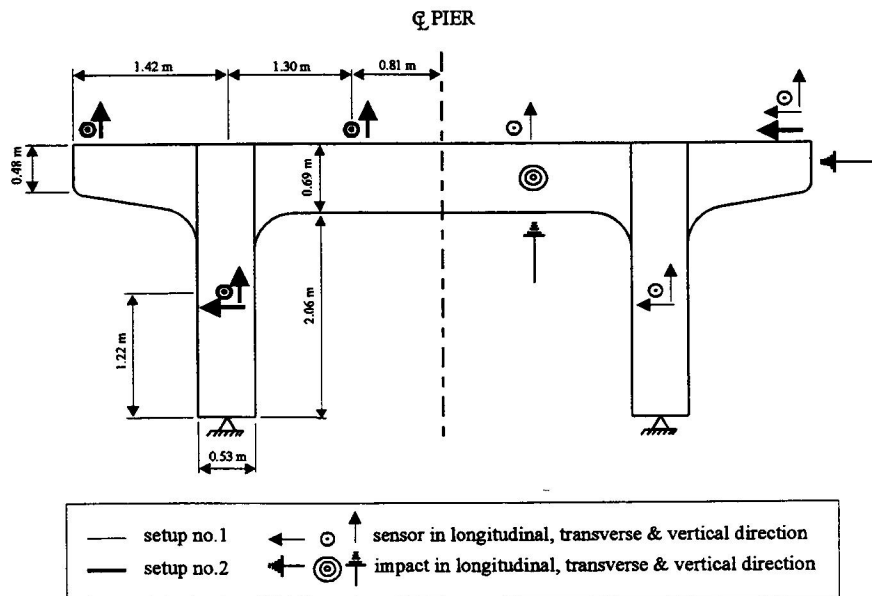


Figure 2. Experimental setup

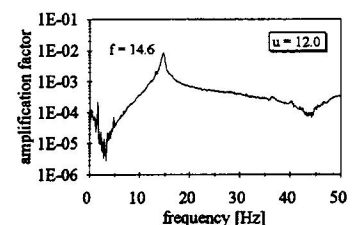
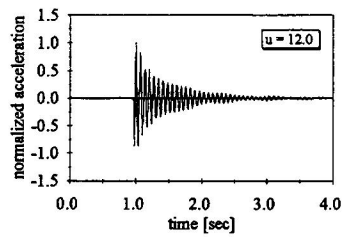
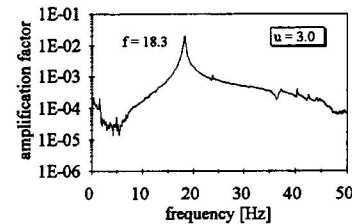
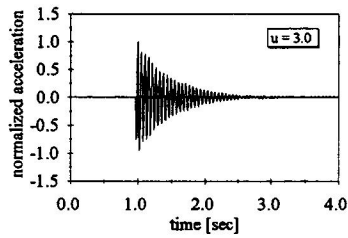
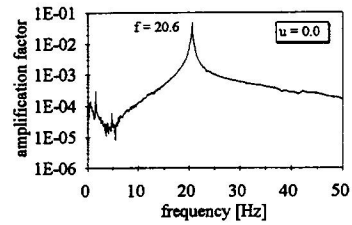
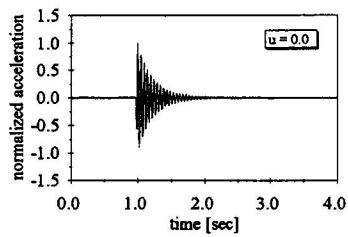


Figure 3. Typical time histories

Figure 4. Typical FRF plots

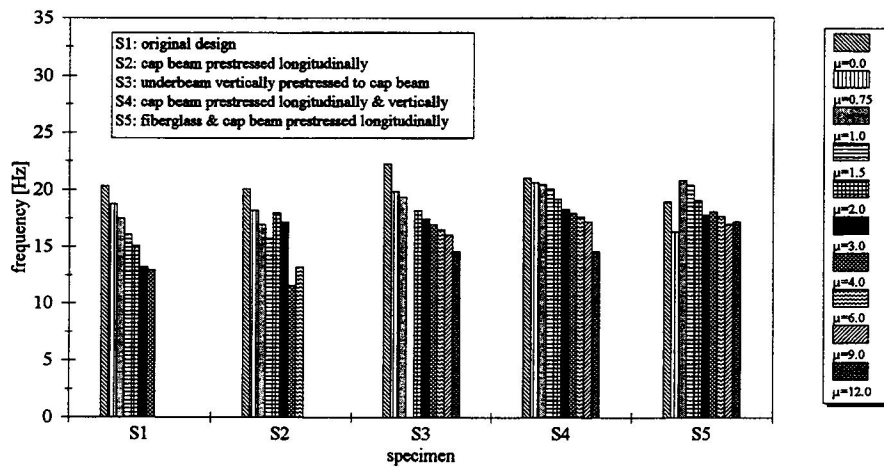


Figure 5. Frequency sensitivity to structural damage

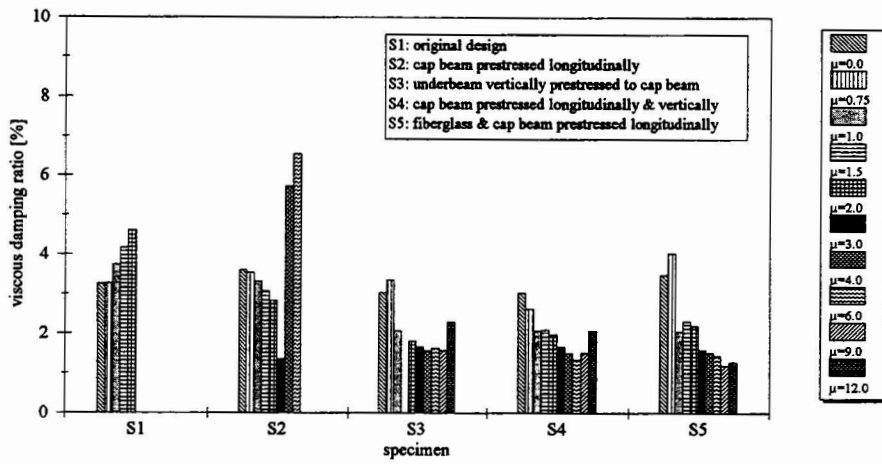


Figure 6. Sensitivity of viscous damping to structural damage

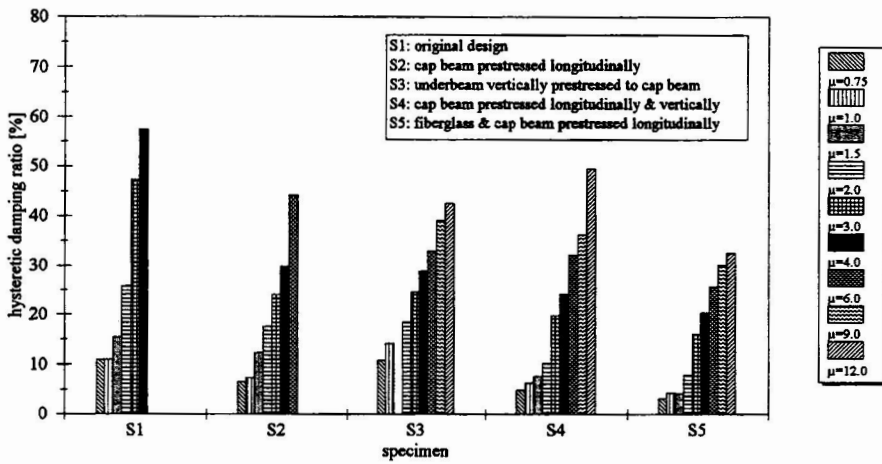


Figure 7. Sensitivity of hysteretic damping to structural damage